Gazi University Journal of Science
GU J Sci
29(2):223-235 (2016)

Experimental Investigation of a Two Dimensional Heat Transfer Performance of Open-Cell Aluminum Foams with the Gis-Based Support Methodology

A. A. SERTKAYA[1,♠], K. DİNCER[2], S. S. DURDURAN[3]

[1]*Necmettin Erbakan University, Seydisehir Vocational High School, Department of Mechanical Education, 42360 Seydisehir, Konya, Turkey*
[2]*Selcuk University, Faculty of Engineering and Architecture, Department of Mechanical Engineering, 42075 Selcuklu, Konya, Turkey*
[3]*Necmettin Erbakan University, Faculty of Engineering and Architecture, Department of Geomatic Engineering, 42075 Meram, Konya, Turkey*

Received: 25/11/2013 *Revised: 10/01/2016* *Accepted: 14/03/2016*

ABSTRACT

In this study, performances ($\Delta T= T_{x,y}- T_i$) of open cell aluminum foams are investigated experimentally for three different situations with GIS (Geographical Information System) based support methodology. In the 1st situation; the conditions were 10 PPI, u=1 and 2 m/s, X=0-200 mm, Y=0-100 mm. In the 2nd situation; 20 PPI, u=1 and 2 m/s, X=0-200 mm, Y=0-100 mm. As in the 3rd situation; 30 PPI, u=1 and 2 m/s, X=0-200 mm, Y=0-100 mm. When the maximum performances of the three situations were compared, the following sequence appeared: $\Delta T_{10,2} < \Delta T_{10,1} < \Delta T_{20,2} < \Delta T_{20,1} < \Delta T_{30,2} < \Delta T_{30,1}$ and the maximum performance was found at the 3rd situation where the data were ($\Delta T_{30,1}$=66.95 ºC; X= 200 mm, Y= 10 mm; $\Delta T_{30,2}$= 40.78 ºC). The empirical correlation of the capacity of non-dimensional performance for the 3rd situation can be expressed as follows $\Delta T_{30,1\ and\ 2} / \left(\Delta T_{30,1\ and\ 2}\right)_{\max} = 6.10^{-8}\ X^4 - 2.10^{-5}\ X^3 + 0.001X^2 - 0.082\,X + 1.459$. Experimental results indicate that the performance depends on porosity density, the magnitude of the air velocity on the test region and the X and Y distances.

Key Words: *Aluminum foam, Geographic Information System (GIS), Thermal performance.*

♠Corresponding author, e-mail: *alisertkaya@hotmail.com*

1. INTRODUCTION

Aluminum foams are the most widely used metal foams in industry. This is due to their useful features such as low density, being corrosion resistant, low melting point and their abundance. Aluminum foams are produced in two different manners, namely open cell (Figuure 1) and closed cell types (Figure 2) [1]. In both open and closed cell aluminum foams; there are spatial volumes at a range of 80% to 95%.

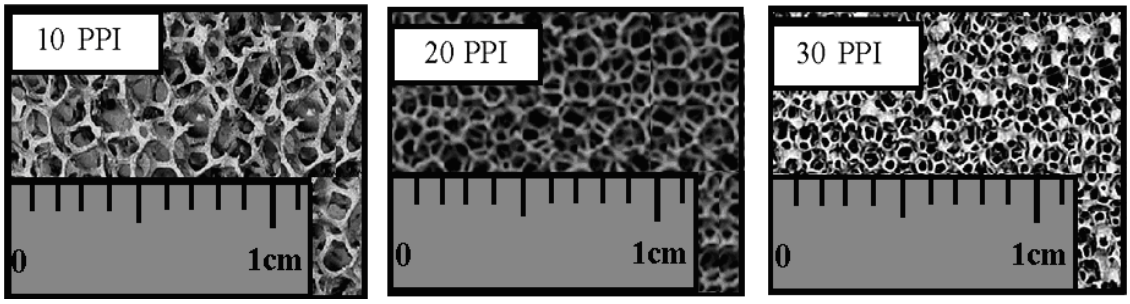

Figure 1. Open cell aluminum foam

Figure 2. Closed cell aluminum foam [1]

So far, there are several published works that deal with experimental and numerical investigations of aluminum foams. Some are briefly mentioned below. Kurtbas et al. [2] carried out a study on exergy transfer in a porous rectangular channel. They found that the effect of open-cell aluminum foam, as a porous medium, in a horizontal rectangular channel with constant wall heat flux on the heat transfer enhancement is quite substantial. The aluminum foam in the channel increases the heat transfer coefficient and outlet temperature of the air. Boomsma et al. [3] studied the dependence of the effective thermal conductivity on the temperature in metal foams, where open-cell aluminum foams were fashioned into heat exchangers for electronic cooling applications. In this way, large amounts of heat can be dissipated.

Sertkaya et al. [4] carried out a study on experimental investigation of thermal performance of aluminum finned heat exchangers and open-cell aluminum foam heat exchangers. They found that for both types of heat exchangers, as the velocity of refrigerant increases, the effectiveness drops and pressure loss increases. The effectiveness was higher at lower Reynolds numbers. It was found that aluminum fin heat exchangers transfer much more heat than their aluminum foam counter parts. Babcsan et al. [5] conducted thermal and electrical conductivity measurements of aluminum foams. Liqun et al. [6] studied cellular structure controllable aluminum foams produced by high pressure infiltration process. Sertkaya [7] investigated the production of aluminum foam as heat exchanger and heat transfer modeling. Kurtbas and Celik conducted experimental investigation on forced and mixed convection heat transfers in a foam-filled horizontal rectangular channel [8].

An information system is a framework that provides answers to questions, from a data resource. A GIS is a special type of information system in which the data source is a database of spatially distributed features and procedures to collect, store, retrieve, analyze, and display geographic data. Geotechnology and geospatial technology are alias names of GIS technology [9]. In the world and our country, GIS has rapidly become an important technology used widely in many fields [10]. GIS technology is becoming an increasingly popular tool for visualization and analyses. GIS has the ability to hold a vast amount of data that can be easily stored, shared analyzed and managed [11]. GIS usually store data from different sources [12]. A GIS is an integration of computer hardware and software which can create manipulate, and analyze a geographically referenced data base to produce new maps or contour maps [13].

In the present study, GIS based support methodology was used to, experimental, study a 2D thermal performance of open cell aluminum foams in three different situations. When the three situations are compared with each other, it is found that;

- ΔT_{max} is $\Delta T_{10,1}$ for 1st situation ΔT=24.30 ^{o}C , u=1 m/s, X=200 mm, Y=10 mm;
- ΔT_{max} is $\Delta T_{20,1}$ for 2nd situation ΔT=28.39 ^{o}C ; u=1 m/s; X = 200 mm, Y=10 mm;
- ΔT_{max} is $\Delta T_{30,1}$ for 3rd situation ΔT=66.95 ^{o}C ; u=1 m/s; X = 200 mm; Y=10 mm,

where $\Delta T_{10,1}$ is the performance in the 1st situation (porosity density = PPI 10, u= 1 m/s). $\Delta T_{20,1}$ is the performance in the 2nd situation (porosity density = PPI 20, u= 1 m/s). $\Delta T_{30,1}$ is the performance in the 3rd (porosity density = PPI 30, u= 1 m/s). The maximum performance in this study was found to be $(\Delta T_{30,1})_{max}$=66.95 ^{o}C, X=200 mm, Y=10 mm.

2. EXPERIMENTAL STUDY

In the present study, two dimensional heat transfer of open cell aluminum foams has been investigated experimentally with the GIS-based support methodology and its experimental system is presented in Figure 3.

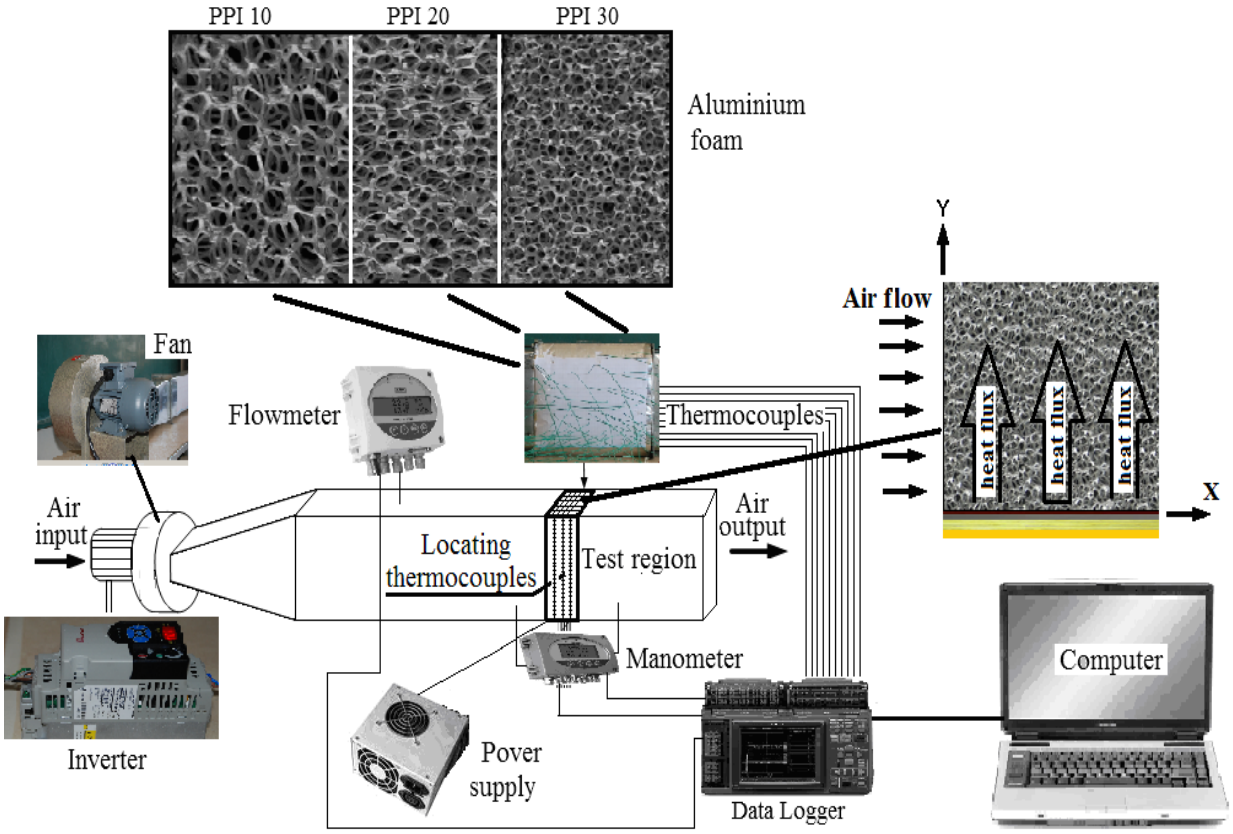

Figure 3. Experimental setup

The experimental set in this study consists of a channel where the test unit is located, aluminum foams having pore densities of 10, 20 and 30 PPI on which their temperature distributions are measured, flexible heaters that enable heating of the foams from lower surfaces towards the upper surfaces, a dimmer which serves as the adjuster of the heater surface temperature and the insulator (glass and rock wool materials) that helps with separating the heaters from the outside environments. In order to maintain homogeneous heat distribution, aluminum plates having dimensions of 100 x 200 x 2 mm were mounted between the flexible heater and the aluminum foams. Air which was used as the cold fluid was blown over the aluminum foams with a blower. The air flow rate was adjusted with an inverter. Inner channel air velocity was read through a digital anemometer while the pressure drop between the inlet and outlet of the test region was determined with a digital manometer. Characteristic features of the measuring tools used in the experimental studies are presented in Table 1.

Table 1. Characteristics and uncertainties of the measurement instruments.

Instrument	Range	Uncertainty
Digital manometer Kimo-CP304	-10000 to +10000Pa	±0.5% and ±10Pa
Thermocouple NiCr-Ni T190-1 (0.5 mm-diameter)	-25 to +400 [^{o}C]	±0.8%
Digital anemometer DCFM8901 CFM	125 to 4900 fpm	±2%

The characteristic values of the PPI 10, 20 and 30 open cell aluminum foams used in the study are shown in Table 2 [14]. When the lower faces of the aluminum foams were heated the air was blown over these foams from their front faces towards their rear sides. Silicon flexible heater was used in heating the aluminum foams.

Table 2. Thermo-physical parameters and dimensions for aluminum foams

Pore density (PPI)	10	20	30
Materials	AlSi7Mg	AlSi7Mg	AlSi7Mg
Porosity, ε	0.90	0.90	0.90
Heat conductivity, k (W/mK)	165	165	165
Density, (kg/m^3)	230	230	230
Specific surface, σ (m^2/m^3)	1200	1500	1800
Height, H (mm)	200	200	200
Length, L (mm)	200	200	200
Width, W (mm)	100	100	100

In order to achieve homogeneous heat transfer to the foams surfaces, a 2 mm thick aluminum plate having the same size as the foams was connected between the flexible heater and the foams. The heater could be adjusted to any required temperature with the help of a regulator. The surface temperatures on the X-Y plane of the aluminum foam were determined with thermocouples. With a help of an inverter air from adjustable fan was blown over the heated aluminum foams from the bottom surfaces towards the rear surfaces. The system was waited until it reached to a steady state, after which the temperature values for the aluminum foams were transferred into a computer with the help of a data logger. System performance was determined by conducting tests on equal lower surface temperatures for system's air velocity of 1 m/s and 2 m/s. The system performance is defined in Eq. 1.

$$\Delta T = T_{x,y} - T_i \quad (1)$$

where $T_{x,y}$ is aluminum foam's temperature on X and Y distance and T_i is the inlet air temperature for the test region. Experiments were conducted at;

- Different porosity density (10, 20, 30 PPI),
- Different test velocity (u= 1 and 2 m/s),
- At different X distances (X=0-200 mm),
- At different Y distances (X=0-200 mm).

3. RESULTS AND DISCUSSIONS

The importance of GIS as an integrating technology is also evident in its pedigree. The development of GIS has relied on innovations made in many different disciplines: Geography, Cartography, Photogrammetry, Remote Sensing, Surveying, Geodesy, Civil Engineering, Statistics, Computer Science, Operations Research, Artificial Intelligence, Demography, and many other branches of the social sciences, natural sciences, and engineering have all contributed. Indeed, some of the most interesting applications of GIS technology discussed below draw upon this interdisciplinary character and heritage [15]. Essentially, there are spatial data (X,Y) in GIS. The data are shown on a geo-reference plane with the help of coordinates, then spatial analysis and query are conducted based on the target. With the analyses conducted, measurements, areas and volumes, proximities, shortest distances and slopes can be determined and used to produce thematic maps.

Distribution of temperature over the surface is shown by the equal temperature curves known as isothermal. And the temperature contours are termed as isothermal curves. These curves can be prepared on daily, monthly or yearly bases. A portion of these curves show real temperature values. These are called real isothermal contours. In these maps, the effects of heights are taken into account. And there are also situations where the

height is taken as zero everywhere and the temperatures are then adjusted accordingly. The contours in such situations are termed as reduced isothermal curves. In order to show the temperature distribution clearly, the steps of the maps are suitably colored. Hot areas are colored red while cold ones are colored blue [16]. Triangulated Irregular Network (TIN) is a surface model used to analyze and display terrain and other types of surfaces [17].

In this study, two dimensional thermal performances of aluminum open cells for three situations were experimentally investigated by using GIS based support methodology and under different porosity densities of 10, 20 and 30 PPI, at velocity different test regions where the initial conditions were: velocities (u= 1 and 2 m/s), different X distances (X=0-200 mm) and different Y distances (Y=0-100 mm). The empirical data were transferred to an Excel file. These data were transferred to ArcGIS9.3, data base which is one of the GIS software. General view was obtained in the given Arc map medium and all data between the $\Delta T_{10,1}$-$\Delta T_{30,2}$ data sets were stored. In order to form TIN, interpolation between the points was conducted to obtain the TIN images for every data set and then isothermal maps were drawn. Isothermal curves were also obtained from the isothermal maps. The different performance results of PPIs application with GIS based support methodology are described as follows:

1st Situation : 10 PPI; u=1 and 2 m/s; X=0-200 mm; Y=0-100 mm (Figures 4-5)

- $(\Delta T_{10,1})_{max} = 24.30\ ^{o}C$, X=200 mm, Y=10 mm,
- $(\Delta T_{10,2})_{max} = 13.02\ ^{o}C$, X=200 mm, Y=10 mm,
- $(\Delta T_{10,2})_{max} < (\Delta T_{10,1})_{max}$,
- ΔT_{max} is $\Delta T_{10,1}$
- $(\Delta T_{10,1})_{min} = 0.68\ ^{o}C$, X=10 mm, Y=100 mm,
- $(\Delta T_{10,2})_{min} = 0.37\ ^{o}C$, X=10 mm, Y=100 mm,
- $(\Delta T_{10,2})_{min} < (\Delta T_{10,1})_{min}$
- ΔT_{min} is $(\Delta T_{10,2})_{min}$.

2nd Situation: 20 PPI; u=1 and 2 m/s; X=0-200 mm; Y=0-100 mm (Figures 6-7).

- $(\Delta T_{20,1})_{max} = 28.39\ ^{o}C$, X=200 mm, Y=10 mm,
- $(\Delta T_{20,2})_{max} = 14.28\ ^{o}C$, X=200 mm, Y=10 mm,
- $(\Delta T_{20,2})_{max} < (\Delta T_{20,1})_{max}$
- ΔT_{max} is $\Delta T_{20,1}$
- $(\Delta T_{20,1})_{min} = 0.73\ ^{o}C$, X=10 mm, Y=100 mm,
- $(\Delta T_{20,2})_{min} = 0.62\ ^{o}C$, X=10 mm, Y=100 mm,
- $(\Delta T_{20,2})_{min} < (\Delta T_{20,1})_{min}$,
- ΔT_{min} is $\Delta T_{20,2}$.

3rd Situation: 30 PPI; u=1 and 2 m/s; X=0-200 mm; Y=0-100 mm (Figures 8- 9).

- $(\Delta T_{30,1})_{max} = 66.95\ ^{o}C$, X=200 mm, Y=10 mm,
- $(\Delta T_{30,2})_{max} = 40.78\ ^{o}C$, X=200 mm, Y=10 mm,
- $(\Delta T_{30,2})_{max} < (\Delta T_{30,1})_{max}$
- ΔT_{max} is $\Delta T_{30,1}$
- $(\Delta T_{30,1})_{min} = 1.35\ ^{o}C$, X=10 mm, Y=100 mm,
- $(\Delta T_{30,2})_{min} = 0.72\ ^{o}C$, X=10 mm, Y=100 mm,
- $(\Delta T_{30,2})_{min} < (\Delta T_{30,1})_{min}$,
- ΔT_{min} is $\Delta T_{30,2}$.

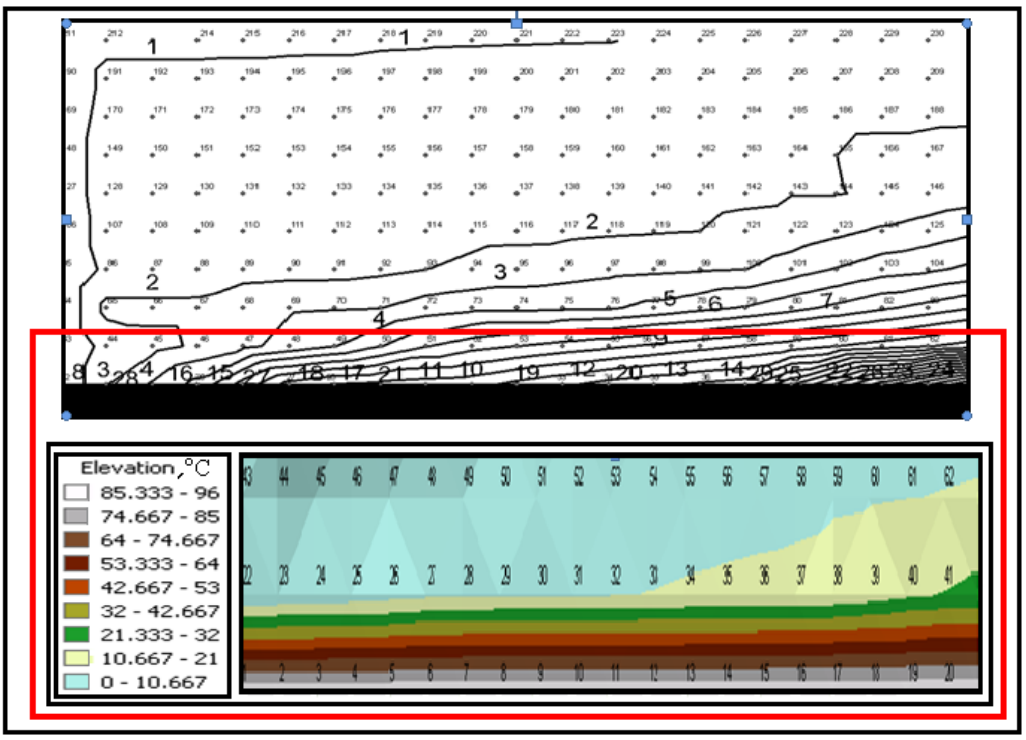

Figure 4. Variation of pore density performance for 10 PPI with respect to X-Y axis and at air velocity of u=1 m/s

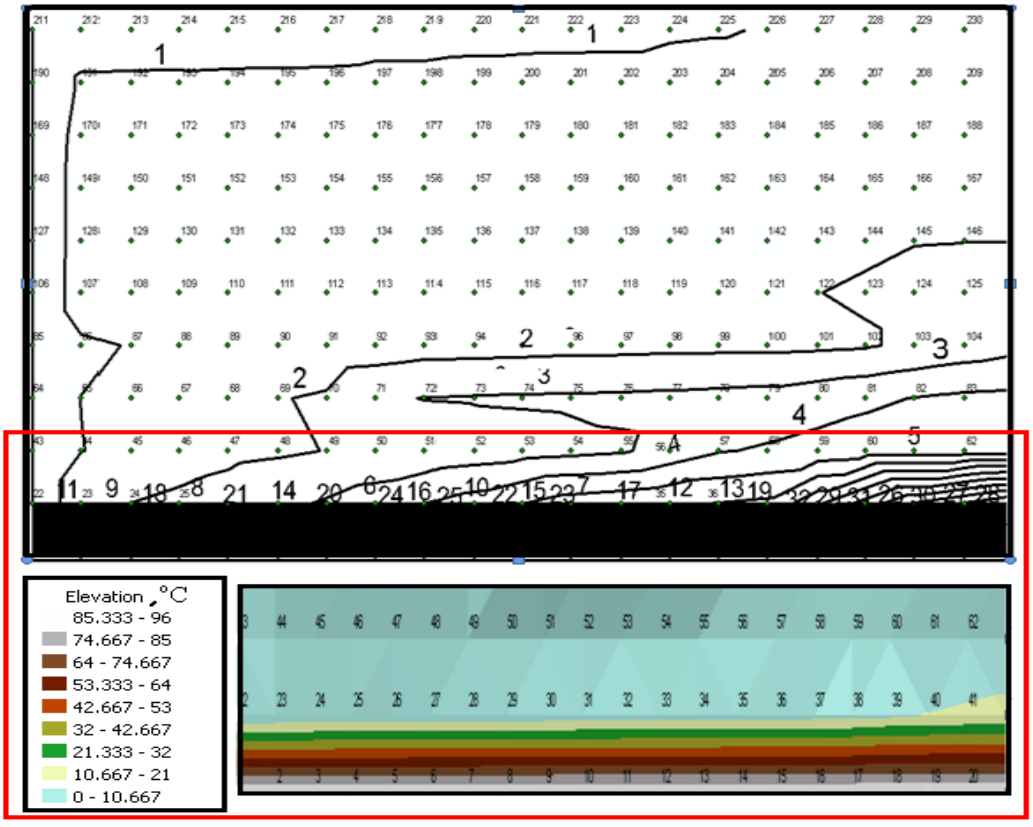

Figure 5. Variation of pore density performance for 10 PPI with respect to X-Y axis and at air velocity of u=2 m/s

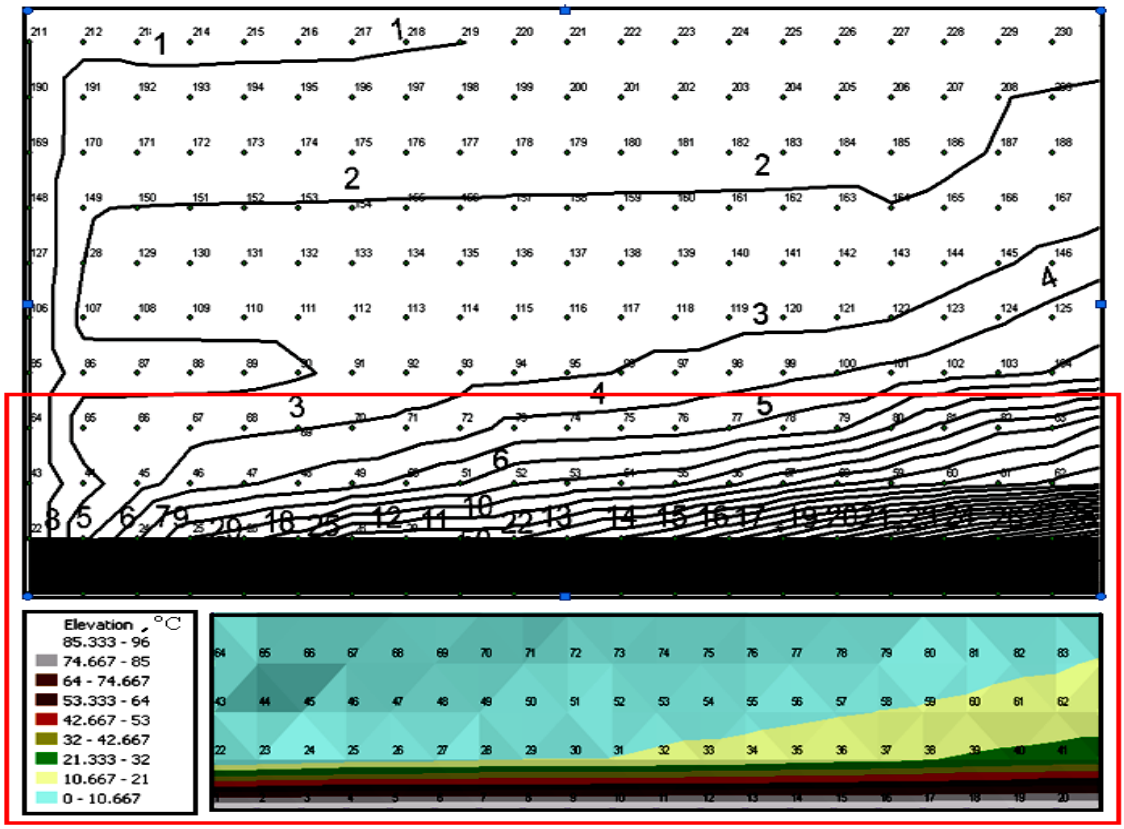

Figure 6. Variation of pore density performance for 20 PPI with respect to X-Y axis and at air velocity of u=1 m/s

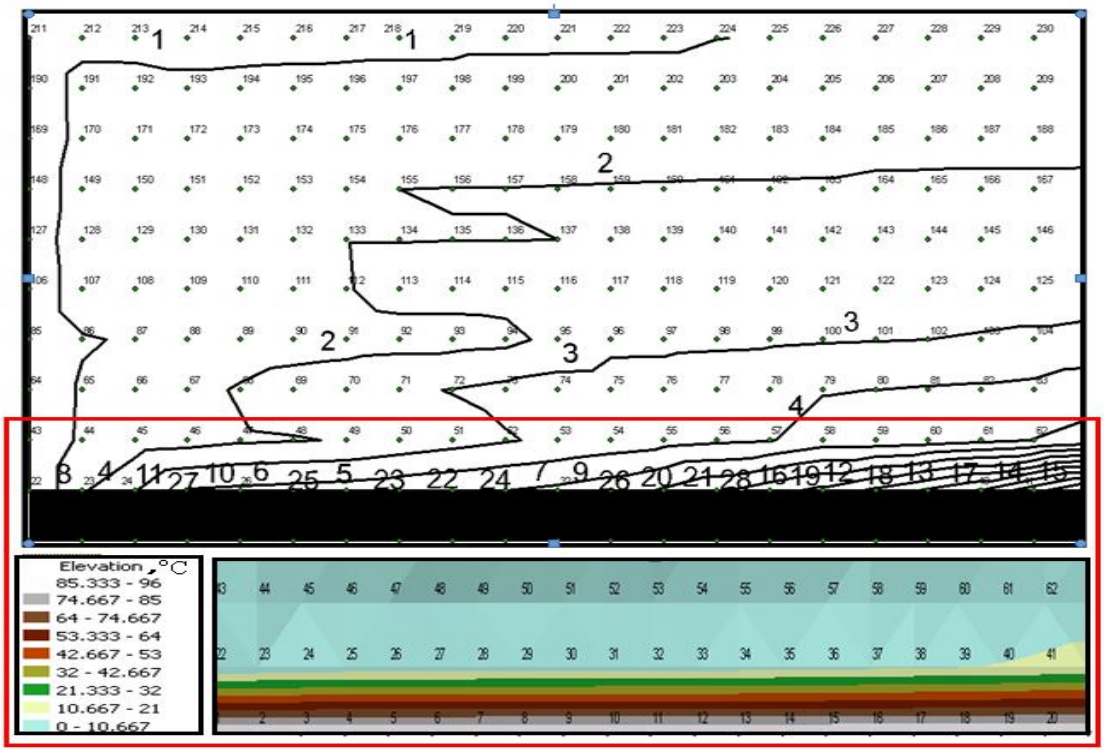

Figure 7. Variation of pore density performance for 20 PPI with respect to X-Y axis and at air velocity of u=2 m/s

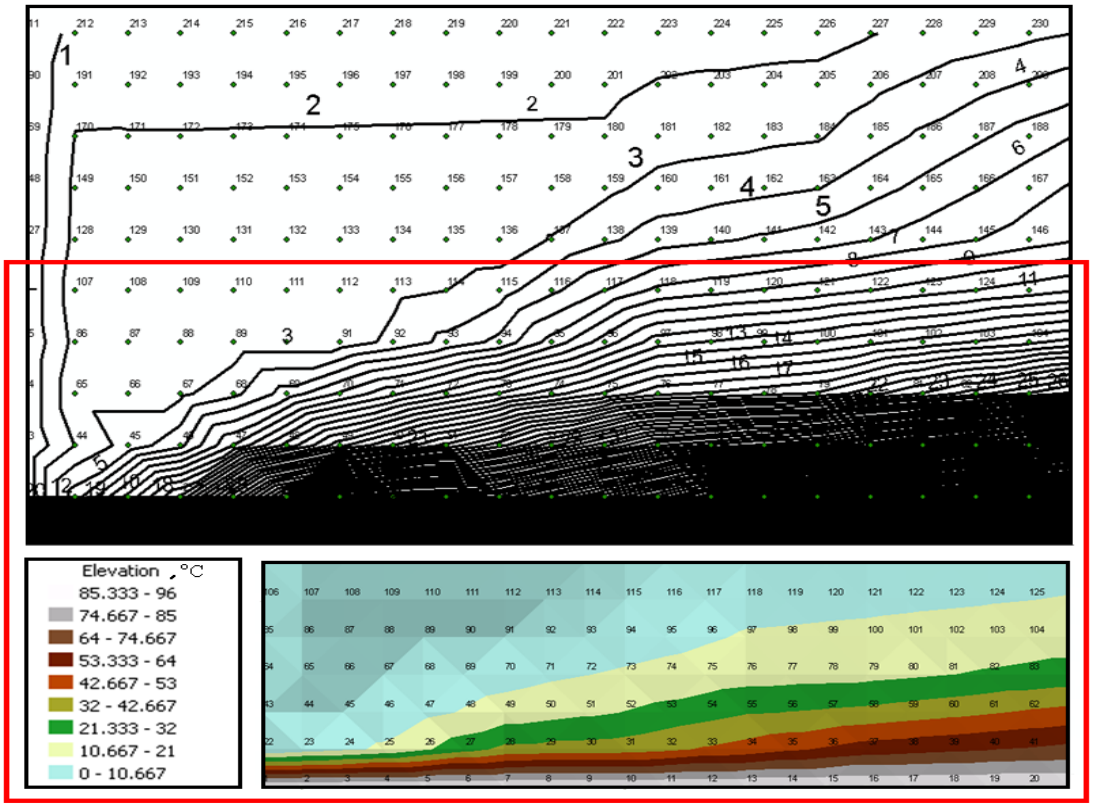

Figure 8. Variation of pore density performance for 30 PPI with respect to X-Y axis and at air velocity of u=1 m/s

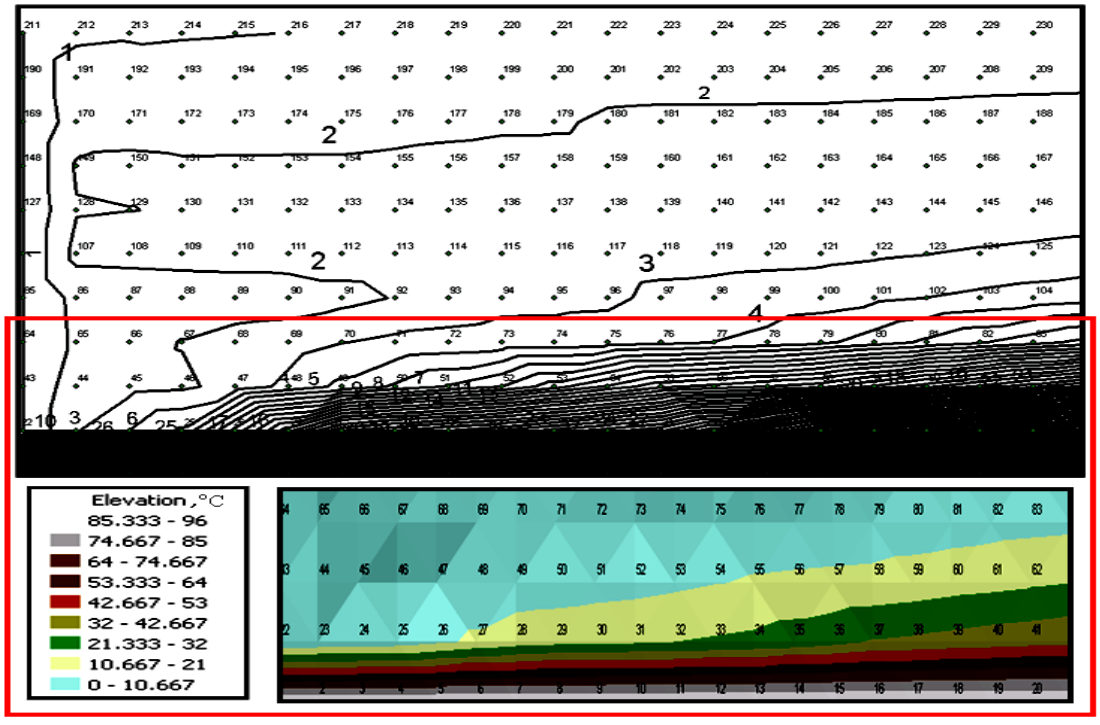

Figure 9. Variation of pore density performance for 30 PPI with respect to X-Y axis and at air velocity of u=2 m/s

When the Figures 4-9 were studied together and compared; the performance of the system was found to be $(\Delta T_{10,2})_{max} < (\Delta T_{20,2})_{max} < (\Delta T_{10,1})_{max} < (\Delta T_{20,1})_{max} < (\Delta T_{30,2})_{max} < (\Delta T_{30,1})_{max}$ and the maximum performance of this study was found to be $(\Delta T_{30,1})_{max}$ = 66.95 °C, X=200 mm, Y=10 mm.

Variations of ΔT with 10, 20, and 30 PPI pore densities on X-Y axis for u = 1 m/s are given in Figure 10, while the same variations where u = 2 m/s are shown on Figure 11. In Figure 10, maximum temperature change is ΔT_{max}=66.95ºC and has occurred at 30 PPI on these coordinates: X=200 mm, Y=10 mm; whereas the minimum temperature change occurred at 10 PPI with these values: ΔT_{min}=0.73 ºC, X=40 mm, Y=100 mm. In Figure 11, the maximum temperature change is exhibited at 30 PPI pore density with a value of ΔT_{max}=40.48 ºC and coordinates of X=200 mm, Y=10 mm while the minimum temperature change is ΔT_{min}=0.43 ºC with these coordinates: X=40 mm, Y=100 mm and taking place at 10 PPI.

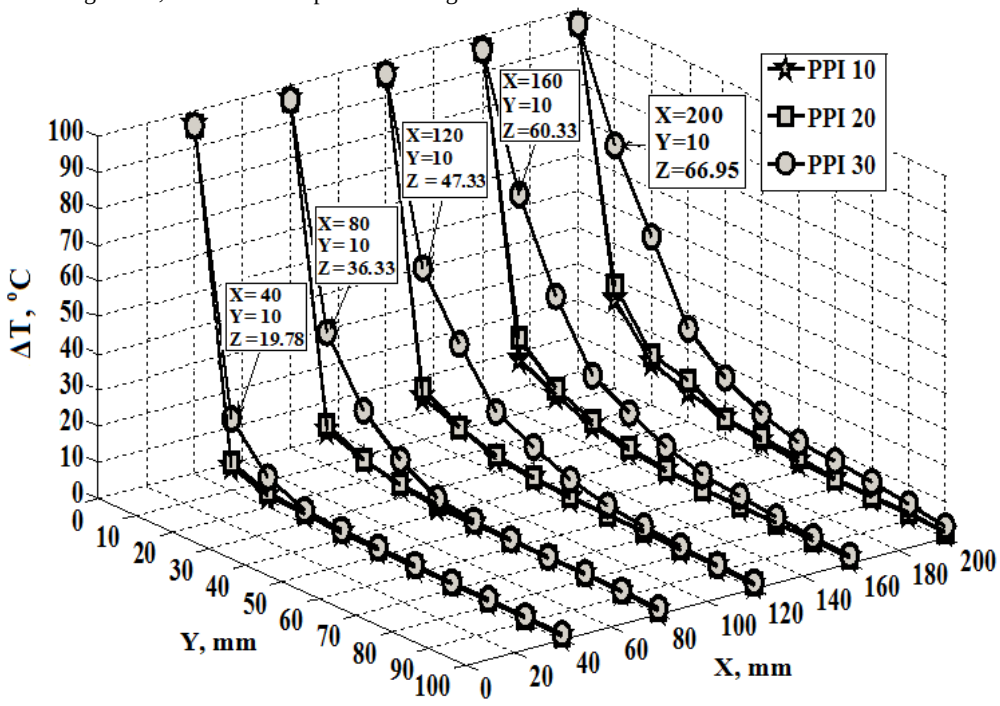

Figure 10. ΔT values along X-Y distance for u=1 m/s

When Figures 4-11 are evaluated together, it is found that ΔT increases as you move along the X axis but decreases as you move towards the Y axis. The temperature differences (ΔT) are higher near the heater and lower as you move away from the heater. The isothermal curves tend to converge on areas with higher temperature changes. It was also found that, while ΔT is at minimum at the entrance of the test region, it reaches peak values outside the test region but at low Y distances. This is due to the advancement of the coils acting as heating fins which absorb heat as they continuously move during air blows within the channel. When comparisons between the temperature drops for the 10, 20 and 30 PPI, on X-Y axes are made, it is found that the drops at air velocity of u=1 m/s are higher than the temperature drops at u = 2 m/s. The reason for this is the fact that air which is the cold fluid stays in contact with the hot coil surfaces for a long time at low air velocities and hence increasing the heat transfer duration. Temperature changes on 30 PPI porous densities are higher than those on 20 PPI and 10 PPI porous densities. This is due to the increase in the distance between the fluid inlet and outlet points existing at increased pore density, and this causes the fluid to pass through narrower channels. This also increases the interval at which air stays in contact with the hot surfaces and thereby increasing the amount of heat the air takes away.

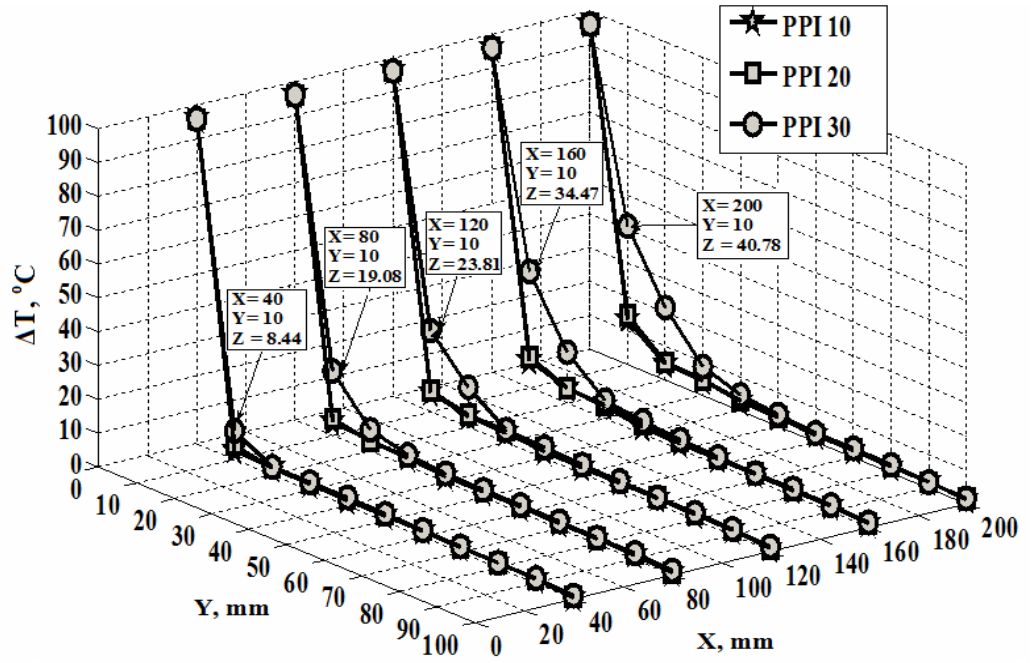

Figure 11. ΔT values along X-Y distance for u=2 m/s

Figure 12 shows variation of non-dimensional heat transfer performance with respect to Y distance for 10 PPI and at X= 200 mm and u = 1m/s and 2 m/s. Figure 13 shows variation of non-dimensional heat transfer performance with respect to Y distance for 20 PPI and at X= 200 mm and u = 1m/s and 2 m/s. while Figure 14 represents variation of non-dimensional heat transfer performance with respect to Y distance for 30 PPI and at X= 200 mm and u = 1m/s and 2 m/s. When Figures 12 through 14 are evaluated together, it is found that non-dimensional performance capacities of open cell aluminum foams depend on pore density, magnitude of the air velocity at the test region and the X and Y distances. In the three aluminum foams, it was experimentally determined that the performances of the foams at u= 1 m/s were more dominant than the performances at u = 2 m/s. The empirical correlation of Figure 12 for the 1st situation is given with Eq. 2 while the empirical correlations for Figures 13 and 14 representing the 2nd and 3rd situations are given with equations 3 and 4 respectively.

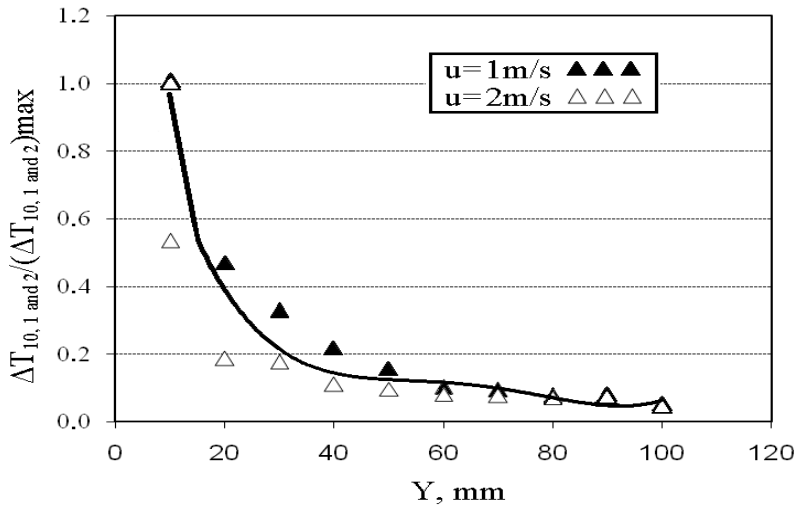

Figure 12. Variation of non- dimensional heat transfer performance for 10 PPI based on Y distance with X= 200 mm and air velocity values of u=1 m/s and u= 2 m/s. This is for the 1st situation

$$\frac{\Delta T_{10,1\ and\ 2}}{\left(\Delta T_{10,1\ and\ 2}\right)_{\max}} = 7.10^{-8}\ X^4 - 2.10^{-5}\ X^3 + 0.001X^2 - 0.080X + 1.375 \quad (2)$$

$$\frac{\Delta T_{20,1\ and\ 2}}{\left(\Delta T_{20,1\ and\ 2}\right)_{\max}} = 9.10^{-8}\ X^4 - 2.10^{-5}\ X^3 + 0.002X^2 - 0.089X + 1.421 \quad (3)$$

$$\frac{\Delta T_{30,1\ and\ 2}}{\left(\Delta T_{30,1\ and\ 2}\right)_{\max}} = 6.10^{-8}\ X^4 - 2.10^{-5}\ X^3 + 0.001X^2 - 0.082X + 1.459 \quad (4)$$

where $\Delta T_{10,1 \text{ and } 2,}$ is the performance in the 1st situation , $\Delta T_{20,1 \text{ and } 2,}$ represents the performance in the 2nd situation and $\Delta T_{30,1\text{and } 2,}$ the performance in the 3rd situation Here $(\Delta T_{10,1 \text{ and } 2})_{max}$ is maximum performance for the 1st situation, $(\Delta T_{20,1 \text{ and } 2})_{max}$ is maximum performance for the 2nd situation and $(\Delta T_{30,1 \text{ and } 2})_{max}$ is the maximum performance for the 3rd situation.

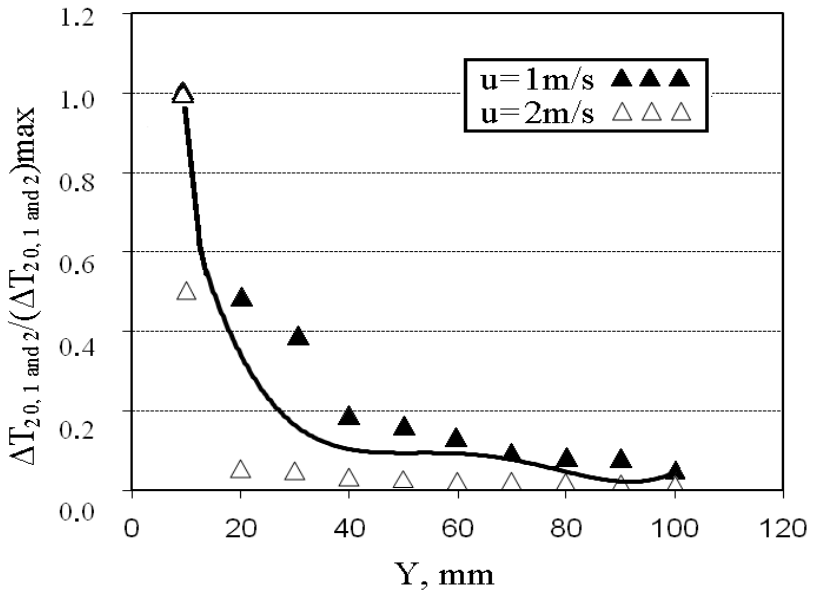

Figure 13. Variation of non- dimensional heat transfer performance for 20 PPI based on Y distance with X= 200 mm and air velocity values of u=1 m/s and u= 2 m/s. This is for the 2nd situation

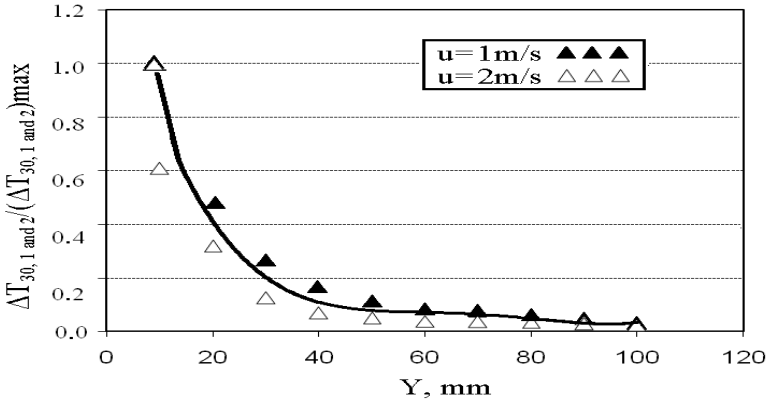

Figure 14. Variation of non- dimensional heat transfer performance for 30 PPI based on Y distance with X= 200 mm and air velocity values of u=1 m/s and u= 2 m/s. This is for the 3rd situation

4. CONCLUSION AND FUTURE WORKS

In this study, GIS based support methodology was used to, experimentally, study a 2D thermal performance of open cell aluminum foams in three different situations and the conclusions drawn in this paper are summarized as follows:

- Lower temperature drops are observed as you move along the Y axis. This is valid for all the three aluminum foams. (Figures 4-11).
- As you move along the X axis, the temperature drops increase for all three aluminum foams with 30 PPI feature experiencing the highest temperature change followed by 20 PPI and 10 PPI hosted the lowest change in temperature.
- Maximum performances for the 1st, 2nd and 3rd situations are respectively given as $\Delta T_{10,1}$(=24.30 ^{o}C), $\Delta T_{20,1}$(=28.39 ^{o}C) and $\Delta T_{30,1}$(=66.95 ^{o}C) (Figures 4-11).
- In this study, it was found that, the performances of celled aluminum foams depend on pore density, air velocity at the test area and the X and Y distances (Figures 12-14).

With this study, it has been proved that GIS-based support methodology can be adapted to studies related to thermal performances. Future works on thermal performances of heat exchangers made of other metal foams like Nickel, Magnesium Lead, Zinc, Copper, Carbon etc. can be conducted with the GIS-based support methodology. An optimum porous density for metals can be determined. The empirical data obtained in this study can be used with other methods like Artificial Neural Networks, Fuzzy Logic and Genetic Algorithms to calculate intermediated pore density values.

ACKNOWLEDGEMENTS

Financial support of this study by the research fund of the Selcuk University under Grant No. BAP 09401075 is gratefully acknowledged.

CONFLICT OF INTEREST

No conflict of interest was declared by the authors.

REFERENCES

[1] Banhart, J., “Aluminum Foams for Lighter Vehicles”, International Journal of Vehicle Design, (2003).

[2] Kurtbas, I., Celik, N., Dincer, I.,” Exergy transfer in a porous rectangular channel”, Energy, 35:451–460, (2010).

[3] Boomsma, K., Poulikakos, D., Ventikos, Y., “Simulations of flow through open cell metal foams using an idealized periodic cell structure”, International Journal of Heat and Fluid Flow, 24:825–834, (2003).

[4] Sertkaya, A.A., Altınışık, K., Dinçer, K., “Experimental investigation of thermal performance of aluminum finned heat exchangers and open-cell aluminum foam heat exchangers”, Experimental Thermal and Fluid Science, 36:86–92, (2012).

[5] Babcsan, N., Meszaros, I., Hegman, N., “Thermal and electrical conductivity measurements on aluminum foams”, Werkstofftech 34:391–394, (2003).

[6] Liqun, M., Zhenlun, S., Deping, H., “Cellular structure controllable aluminum foams produced by high pressure infiltration process”, Department of Materials Science and Engineering, Southeast University, Nanjing, Pergamon 41:785–789, (1999).

[7] Sertkaya, A.A., “The production of aluminum foam as heat exchanger & heat transfer modeling”, PhD thesis, Department of Mechanical Engineering, Graduate School of Natural and Applied Sciences, Selcuk University, Konya, Turkey, (2008).

[8] Kurtbas, I., Celik, N., “Experimental investigation of forced and mixed convection heat transfer in a foam-filled horizontal rectangular channel”, International Journal of Heat and Mass Transfer, 52:1313–1325, (2009).

[9] Uzair, M.S., “GIS tools for water, wastewater, and storm water systems”, New Ages International Publishers, New Delhi, (2005).

[10] Dilek, E.F., Sahin, S., Yılmazer, I., “Afforestation areas defined by GIS in Gölbası specially protected area Ankara/Turkey”, Environmental Monitoring and Assessment, 144(1-3): 251–259, (2008).

[11] Durduran, S.S., “A Decision Making System to Automatic Recognize of Traffic Accidents on the basis of a GIS Platform”, Expert Systems With Applications 37(12):7729-7736, (2010).

[12] Burrough, P.A., McDonnell, R.A., “Principle of Geographical Information Systems”, Oxford University Press, New York, (1998).

[13] Yomralıoglu, T., “Geographical Information System: Basic Concepts and Applications”, Second Edition, Seçil Offset, Istanbul, (2002).

[14] www.m-pore.de, (2012).

[15] Fazal, S., GIS Basic. New Age International Limited Publishers, New Delhi, (2008).

[16]www.okulweb.meb.gov.tr/01/17/972369/Dökümanlar/SICAKLIK.pdf, (2012).

[17] Shewchuk, J.R., Delaunay refinement algorithms for triangular mesh generation. Computational Geometry: Theory and Applications, 22 (3):21–74, (2002).

NOMENCLATURE

ΔT	temperature difference ($\Delta T= T_{x,y}- T_i$) (^oC)
T_i	test region inlet temperature (^oC)
$T_{x,y}$	specimen temperature along X and Y distances (^oC)
u	in-channel inner air velocity (m/s)
PPI	number of pores per inch
ΔT_{max}	maximum performance (^oC)
ΔT_{min}	minimum performance (^oC)
$\Delta T_{10,1}$	performance of 10 PPI; u=1 m/s (^oC)
$\Delta T_{10,2}$	performance of 10 PPI; u=2 m/s (^oC)
$\Delta T_{20,1}$	performance of 20 PPI; u=1 m/s (^oC)
$\Delta T_{20,2}$	performance of 20 PPI; u=2 m/s (^oC)
$\Delta T_{30,1}$	performance of 30 PPI; u= 1 m/s (^oC)
$\Delta T_{30,2}$	performance of 30 PPI; u=2 m/s (^oC)
$(\Delta T_{10,1})_{max}$	maximum performance of 10 PPI; u= 1 m/s (^oC)
$(\Delta T_{10,2})_{max}$	maximum performance of 10 PPI; u= 2 m/s (^oC)
$(\Delta T_{20,1})_{max}$	maximum performance of 20 PPI; u= 1 m/s (^oC)
$(\Delta T_{20,2})_{max}$	maximum performance of 20 PPI; u= 2 m/s (^oC)
$(\Delta T_{30,1})_{max}$	maximum performance of 30 PPI; u= 1 m/s (^oC)
$(\Delta T_{30,2})_{max}$	maximum performance of 30 PPI; u= 2 m/s (^oC)
$(\Delta T_{10,1})_{min}$	minimum performance of 10 PPI; u= 1 m/s (^oC)
$(\Delta T_{10,2})_{min}$	minimum performance of 10 PPI; u= 2 m/s (^oC)
$(\Delta T_{20,1})_{min}$	minimum performance of 20 PPI; u= 1 m/s (^oC)
$(\Delta T_{20,2})_{min}$	minimum performance of 20 PPI; u= 2 m/s (^oC)
$(\Delta T_{30,1})_{min}$	minimum performance of 30 PPI; u= 1 m/s (^oC)
$(\Delta T_{30,2})_{min}$	minimum performance of 30 PPI; u= 2 m/s (^oC)
$\Delta T_{10,1 \text{ and } 2}$	performance of 1st situation (^oC)
$\Delta T_{20,1 \text{ and } 2}$	performance of 2nd situation (^oC)
$\Delta T_{30,1 \text{ and } 2}$	performance of 3rd situation (^oC)
$(\Delta T_{10,1 \text{ and } 2})_{max}$	maximum performance of 1st situation (^oC)
$(\Delta T_{20,1 \text{ and } 2})_{max}$	maximum performance of 2nd situation (^oC)
$(\Delta T_{30,1 \text{ and } 2})_{max}$	maximum performance of 3rd situation (^oC)